Methods xxx (xxxx) xxx

Contents lists available at ScienceDirect

Methods

journal homepage: www.elsevier.com/locate/ymeth

Rapid and efficient cataract gene evaluation in F0 zebrafish using CRISPR-Cas9 ribonucleoprotein complexes

Duran Zhao [a], Johanna L. Jones [a], Robert J. Gasperini [b], Jac C. Charlesworth [a], Guei-Sheung Liu [a,c,1], Kathryn P. Burdon [a,d,1,*]

[a] Menzies Institute for Medical Research, University of Tasmania, Hobart, Tasmania, Australia
[b] School of Medicine, University of Tasmania, Hobart, Tasmania, Australia
[c] Ophthalmology, Department of Surgery, University of Melbourne, East Melbourne, Victoria, Australia
[d] Department of Ophthalmology, Flinders University, Bedford Park, South Australia, Australia

ARTICLE INFO

Keywords:
CRISPR
Cas9
Ribonucleoprotein (RNP) complex
Genome editing
Cataract
Zebrafish

ABSTRACT

Cataract is the leading cause of blindness worldwide. Congenital or paediatric cataract can result in permanent visual impairment or blindness even with best attempts at treatment. A significant proportion of paediatric cataract has a genetic cause. Therefore, identifying the genes that lead to cataract formation is essential for understanding the pathological process of inherited paediatric cataract as well as to the development of new therapies. Despite clear progress in genomics technologies, verification of the biological effects of newly identified candidate genes and variants is still challenging. Here, we provide a step-by-step pipeline to evaluate cataract candidate genes in F0 zebrafish using CRISPR-Cas9 ribonucleoprotein complexes (RNP). Detailed descriptions of CRISPR-Cas9 RNP design and formulation, microinjection, optimization of CRISPR-Cas9 RNP reagent dose and delivery route, editing efficacy analysis as well as cataract formation evaluation are included. Following this protocol, any cataract candidates can be readily and efficiently evaluated within 2 weeks using basic laboratory supplies.

1. Introduction

Cataract is an opacity of the transparent crystalline lens in the eye that interferes with the path and refraction of light to the retina. It is the principal cause of reversible visual impairment or blindness worldwide [1]. While cataract in adults is usually treatable with access to surgery, congenital or paediatric cataract can lead to life-long irreversible vision impairment or blindness, despite best attempts at treatment. A significant proportion of paediatric cataract is inherited and it often occurs alongside other syndromic features. Identifying the causative genes for inherited paediatric cataract can improve diagnostic accuracy through facilitating genetic testing. Gene identification can also improve understanding of the molecular mechanisms underlying cataractogenesis which may facilitate the development of medical therapy and individualized treatment [2]. So far, more than 40 genes have been linked to congenital or early-onset cataract [3–5] and they account for 60–70% of children with the disease [6–8]. However, significant challenges exist for identifying additional genes. Genome sequencing technologies are able to identify candidate variants, but validating these genes in multiple families is increasingly difficult for rare genetic causes of disease. Medium to high throughput techniques for evaluating the role of candidate genes in cataract formation are required.

These human cataract candidate genes can be verified in animal models. Gene knockout models that display cataract formation provide strong evidence that a candidate gene is important in lens biology and cataract development. Several animal models have been used in cataract research, including mice, rats, rabbits, dogs, and zebrafish. However, the relatively small number of offspring and long generation period limit the application of mammalian models. In contrast, zebrafish (*Danio rerio*) become an outstanding model system due to a number of advantages. Their rapid development and simple husbandry enable the generation of large numbers of fish for genetic research work from a single mating. Zebrafish embryos develop externally and remain transparent for the first few days of development, providing technical advantages for embryo microinjection. The eyes of the embryos are relatively large [9] and become functional by 3 days-post-fertilization (dpf) [10], allowing for

* Corresponding author at: 17 Liverpool Street (Private Bag 23), Hobart, Tas 7000, Australia.
E-mail address: kathryn.burdon@utas.edu.au (K.P. Burdon).
[1] These senior authors contributed equally to this work.

https://doi.org/10.1016/j.ymeth.2020.12.004
Received 5 November 2020; Received in revised form 22 December 2020; Accepted 29 December 2020
Available online 6 January 2021

the observation of lens morphology at an early stage. The genome of zebrafish has been sequenced and annotated. Around 70% of human genes have functional orthologs in zebrafish [11]. This high level of homology to humans means that most human genes can be interrogated in zebrafish and the functions of those genes are largely similar between the two species.

Clustered regularly interspaced short palindromic repeat (CRISPR)-Cas9 nuclease system has become a widely used targeted gene editing technology in zebrafish models. Its advantages over other methods such as zinc finger nucleases (ZFNs) and transcription activator-like effector nucleases (TALENs) include easy design processes and rapid synthesis of reagents. Morpholinos (MOs) have been used extensively for temporary knockdown of genes in zebrafish, but CRISPR-Cas9 provides a permanent genetic modification with relatively low off-target effects. The system is comprised of guide RNA (gRNA) and Cas9 nuclease, which are combined to form a ribonucleoprotein (RNP) complex. The gRNA consists of a target-specific CRISPR RNA (crRNA) and a universal trans-activating RNA (tracrRNA). The crRNA is designed to be complementary to the target DNA site, a 20 base pair sequence next to a protospacer adjacent motif (PAM) [12]. The gRNA forms a complex with the specific target site, directing the Cas9 nuclease to that locus. Once at the appropriate site, Cas9 nuclease can induce double-strand breaks (DSB), triggering non-homologous end joining (NHEJ) to repair the break. The error-prone NHEJ can produce small insertions or deletions between the end of the broken DNA strands, resulting in efficient mutagenesis [12–14].

Although many articles have described disease modelling in zebrafish, specific protocols for evaluation of cataracts in CRISPR-Cas9 edited zebrafish have not been reported. In this article, we provide a rapid and highly efficient method for evaluating cataract candidates in F0 zebrafish using CRISPR-Cas9 RNP. Detailed pipelines of CRISPR-Cas9 RNP design and formulation, microinjection, dose and delivery route optimization of CRISPR-Cas9 RNP, editing efficacy analysis as well as cataract formation evaluation are included.

2. Overview

To better describe the pipeline of using CRISPR-Cas9 RNP to evaluate cataract genes in F0 zebrafish, we use *HTR1F* (5-hydroxytryptamine receptor 1F) as an example cataract candidate gene to illustrate the methods applied in this article. The *HTR1F* protein is a G-protein coupled serotonin receptor. Serotonin is crucial in lens transparency [15] and increased serotonin level has been shown to lead to lens opacities in rats [16]. The data presented in Section 4.4 and lens images shown in Section 4.5.2 were generated from *HTR1F* knockout experiments. Fig. 1 illustrates the overall experimental workflow.

3. Materials

3.1. Reagents and equipment

The reagents and equipment utilized in this protocol are summarized in Table 1 and Table 2.

3.1.1. Reagent setup

3.1.1.1. E2 embryo media with methylene blue. The 0.5x E2 with 0.5 mg/l Methylene Blue working solution was prepared following the Zebrafish International Resource Center (ZIRC) protocol: https://zebrafish.org/wiki/protocols/nursery. The final concentrations of E2 media components are: 7.5 mM NaCl, 0.25 mM KCl, 0.5 mM MgSO4, 75 μM KH2PO4, 25 μM Na2HPO4, 0.5 mM CaCl2, and 0.35 mM NaHCO3.

3.1.1.2. 1x PTU (200 μM) egg water. Add 0.076 g PTU (1-phenyl-2-thiourea) to 50 ml autoclaved Milli-Q water to prepare a 50x PTU (10,000 μM) stock solution. Store the 50x PTU stock solution at room temperature. Prepare fresh 1x PTU (200 μM) egg water each time as needed by diluting 50x PTU stock solution 50 times with E2 embryo media with Methylene Blue.

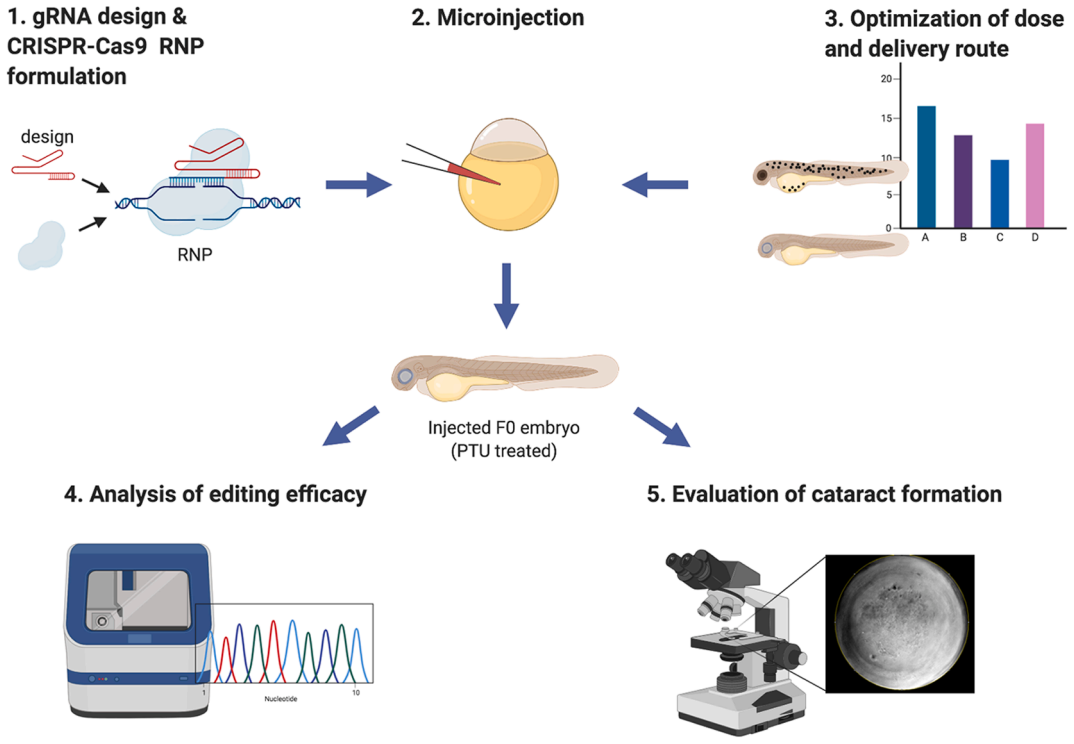

Fig. 1. Overview of the main steps of the cataract gene evaluation pipeline. Each step corresponds to a section of the protocol with the same title.

Table 1
Reagents used in this protocol.

Item	Supplier	Catalogue No.
NaCl, KCl, $MgSO_4$, KH_2PO_4, Na_2HPO_4, $CaCl_2$, $NaHCO_3$. KCl powder	Sigma-Aldrich	–
Methylene Blue	AQUASONIC	PL084
Alt-R® CRISPR-Cas9 crRNA	IDT	–
Alt-R® CRISPR-Cas9 tracrRNA	IDT	1072533
Alt-R® S.p.HiFi Cas9 Nuclease V3	IDT	1081060
IDTE pH 7.5 (1X TE Solution)	IDT	11-01-02-02
1 M HEPES buffer	Sigma-Aldrich	H3375
Nuclease-Free Duplex buffer	IDT	11-01-03-01
PTU (1-phenyl-2-thiourea)	Sigma-Aldrich	P7629
Tricaine methanesulfonate	Glentham Life Sciences	GE5936
Phire Tissue Direct PCR Master Mix	Thermo Scientific	F170s
Agarose powder	Bioline	BIO-41025
TAE buffer (Tris-acetate-EDTA) (50X)	Thermo Scientific	B49
HyperLadder™ 100 bp	Meridian Bioscience	BIO-33056
AMPure XP beads	Beckman Coulter	A63880
CleanSEQ Dye-Terminator Removal kit	Beckman Coulter	A29151
BrilliantDye™ Terminator (v3.1) Cycle Sequencing kit	NimaGen	BRD3-1000
BigDye™ Terminator v1.1 & v3.1 5X Sequencing Buffer	Thermo Scientific	4336699
Ethanol	Sigma-Aldrich	E7023

NOTE:

- PTU is highly toxic by ingestion and is a skin sensitizer. Weigh and prepare the PTU in a fume hood and always have gloves on during use.

3.1.1.3. Alt-R CRISPR-Cas9 crRNA, tracrRNA and Cas9 nuclease aliquots. The CRISPR oligos are usually received dehydrated. Resuspend the Alt-R CRISPR-Cas9 crRNA and tracrRNA in IDTE buffer to final concentrations of 100 μM each. Store the rehydrated CRISPR oligos and S.p.HiFi-Cas9 nucleases according to supplier instructions. At the time of these experiments, we aliquoted crRNA, tracrRNA and S.p.HiFi-Cas9 Nuclease into 2 μl small stocks and stored at −20 °C to reduce unnecessary freeze–thaw cycles.

Table 2
Equipment required for this protocol.

Item	Supplier	Catalogue No.
Standard microcentrifuge tubes, 1.5 ml	Labcon	#3039-560-000
RNase-free microfuge tubes, 1.5 ml	Thermo Scientific	AM12400
Filtered sterile pipette tips	Labcon	–
Desktop microcentrifuges	Bioline Global	SF7000
Vortex mixer	Ratek	IC-VM1
Block heater	Ratek	DBH200
Capillary glass (1.0 mm × 0.58 mm × 10 cm)	Harvard Apparatus	GC100F-10
Micropipette puller	Sutter Instrument	P-87
Pico-liter injector	Warner Instruments	PLI-10
Petri dish	NEST Scientific	752001
Nunc™ glass base dish (27 mm)	Thermo Scientific	150682
Incubator	Nüve	EN025
Stereomicroscope	Olympus	SZX16
Inverted microscope	Nikon	Eclipse Ti
S-Series compact USB 2.0 camera	Mightex	SCE-B013-U
sCMOS camera	Andor	Zyla 4.2 PLUS
Veriti™ 96-well Thermal cycler	Applied Biosystems	4375786
PowerPac™ basic power supply	Bio-Rad	1645050
Magnetic plate	ALAPAQUA	A001322
3500 Genetic Analyzer	Thermo Scientific	A27772

3.1.1.4. Cas9 working buffer (20 mM HEPES; 150 mM KCl, pH 7.5). Mix the following:

Component	Amount
1 M HEPES buffer	300 μl
KCl powder	0.168 g
RNase-free H_2O	14.7 ml
Final volume	15 ml

After KCl powder completely dissolves in the solution, aliquot the Cas9 working buffer into 1 ml stocks and store at 4 °C.

3.2. Zebrafish maintenance and breeding

AB strain zebrafish (source: Zebrafish International Resource Center (ZIRC)) were housed in a circulating water system under standard conditions [17], with a daily cycle of 14 h light/10 h dark. Embryos were obtained from the natural pairwise spawns of the wildtype AB zebrafish and were collected and raised in an incubator at 28.5 °C in E2 media with Methylene Blue until 5 dpf. The animal research in this study was approved by the University of Tasmania Animal Ethics Committee (project number: A0017743) in accordance with the Australian National Health and Medical Research Council Code of Practice for the Care and Use of Animals for Scientific Purpose.

4. Methods

4.1. gRNA design and CRISPR-Cas9 RNP formulation

4.1.1. gRNA design

The first and most critical step is the design of gRNA. The editing efficiencies of each gRNA can vary greatly, thus a well-designed gRNA is essential for successful CRISPR-Cas9-based gene disruptions. It is worth noting that zebrafish frequently have more than one ortholog of human genes [11]. For example, the *HTR1F* gene has two orthologs in the zebrafish genome, *HTR1Fa* and *HTR1Fb*. Collect the genomic DNA sequence, transcripts and protein information of all the orthologs of your target gene before starting gRNA design. There are multiple zebrafish genomic resources including Zebrafish Information Network (ZFIN) (http://zfin.org/), Ensembl (http://www.ensembl.org/Danio_rerio/Info/Index), UCSC genome browser (https://genome.ucsc.edu/) and NCBI zebrafish genome (https://www.ncbi.nlm.nih.gov/). Several CRISPR design tools are available online, such as CHOPCHOP (https://chopchop.cbu.uib.no/), CRISPOR (http://crispor.tefor.net/) and E-CRISP (http://www.e-crisp.org/E-CRISP/). For beginners we recommend CHOPCHOP, as it is simple and intuitive. Here we use CHOPCHOP as an example to explain the steps of gRNA design.

1. Input the gene identifiers or genomic coordinates or paste the genomic sequence of your target gene into CHOPCHOP, specify the organism and CRISPR mode to be "Danio rerio (danRer11/GRCz11)" and "CRISPR-Cas9" "knock-out". Under the "Options", by default, the target region, PAM sequence and number of mismatches of predicted off-targets have been set to "coding region", "NGG" and "up to 3" respectively. These parameters can be adjusted according to individual needs. After setting, click "Find Target Sites!" to perform guide search.
2. A list of candidate gRNAs with relevant information such as target sequence, genomic location, number and type of predicted off-targets, GC content and efficiency score should be displayed. Detailed information of predicted off-targets including location, number of mismatches, and sequence can be found by clicking on an individual guide. Based on this information, select suitable gRNAs according to the principles below:

- **Position.** It is recommended that the target sites are located within the most upstream exon that is conserved across all target transcripts

of the gene of interest. This is most likely to generate frameshift mutations and early termination of the protein sequence. Alternatively, gRNAs can be designed to target exons encoding known functional protein domains. In this way, the protein function could be disrupted even with non-frameshift alleles.

- **Editing efficiency.** Select gRNAs with the highest on-target efficiency and the fewest predicted off-targets. Generally, guides with predicted off-targets containing three or fewer mismatches to the target sequence should be avoided [13]. When multiple gRNAs have similar on and off-target efficiencies, priority is given to gRNAs with off-target loci on chromosomes other than the one that the target gene resides, or in non-coding regions (e.g. intergenic) that are unlikely to have impacts on gene expression.
- **Number.** It has been shown that targeting a single locus in a coding region only generates biallelic loss-of-function alleles 44% of the time, however, targeting a coding region at two, three, or four independent loci generates biallelic loss of function variants 79%, 93%, and 98% of the time respectively [14]. To increase the success rate of introducing mutations and producing loss of protein function, we recommend designing 2 to 4 gRNAs for each target gene. Nonetheless, it is suggested the total number of gRNAs injected per embryo does not exceed 8, otherwise it may affect the survival and development of zebrafish embryos as well as increase the off-target effects [14]. The exact number of gRNAs to be injected into the zebrafish embryo depends on which gene is being targeted, the number of orthologs of the target gene, and how many genes are to be targeted simultaneously.
- **GC% of the guide sequence.** A previous study has identified that gRNAs with over 50% GC content exhibit high mutagenesis activity [18].

3. Order CRISPR oligos. The fully functional gRNA consists of the target-specific crRNA (designed above) and the tracrRNA with a universal sequence. The two components can be ordered pre-synthesized into the gRNA which can provide greater stability for challenging experimental conditions. Alternatively, for greater flexibility, they can be ordered individually and assembled in house.

NOTE:

- The gRNA target sequences should be verified by Sanger sequencing in the strain of fish to be used in your experiment. It is possible, depending on the strain and source of the fish, that polymorphisms are present compared to the reference used to design the gRNAs. Even a single base mismatch can significantly reduce the targeting efficiency of the CRISPR system [19].
- To eliminate the interference caused by CRISPR protein as well as injection-induced defects, it is necessary to involve a negative control in the experiments. gRNA against a non-existent gene in the zebrafish genome such as *LacZ*, a gene of *E. coli*, can be designed as a negative control. Align the target sequence of your negative control to the zebrafish genome to make sure there is no target in the zebrafish, and check the predicted off-targets of the negative control to avoid targeting your gene of interest.

4.1.2. CRISPR-Cas9 RNP formulation

Two approaches have been commonly used to construct the CRISPR-Cas9 system for *in vivo* microinjection. Early methods co-inject gRNA and Cas9 mRNA into zebrafish embryos. With the proliferation of CRISPR-Cas9 reagents and suppliers, the more handy and cost-effective way is to directly deliver gRNA and Cas9 protein as RNP complex. Compared to mRNA-mediated delivery, RNP has the advantages of high stability, fast onset, and more importantly, by skipping the transcription process, it is likely to reduce genetic mosaicism due to Cas9 expression delay [20,21]. The protocol below used the Alt-R CRISPR-Cas9 system to synthesize CRISPR-Cas9 RNP and has been adapted from instructions provided by IDT (online instructions: Zebrafish embryo microinjection: Ribonucleoprotein delivery using the Alt-R CRISPR-Cas9 System).

1. On the day of injection, thaw crRNA, tracrRNA and HiFi-Cas9 nuclease stocks at room temperature.
2. Preheat the heat block to 95 °C.
3. Prepare 9 μM gRNA working solution by mixing the following components:

Component	Volume (μl)
100 μM Alt-R® CRISPR-Cas9 crRNA	0.9
100 μM Alt-R® CRISPR-Cas9 tracrRNA	0.9
Nuclease-Free Duplex buffer	8.2
Final volume	10

In the case of multiple crRNAs, mix the crRNAs equally while keeping the total amount of crRNAs constant. The volumes provided here are the optimized results generated in our experiments (see Section 4.3). The user can adjust the volumes as required.

4. Heat gRNA working solution at 95 °C for 5 min.
5. Remove the working solution from the heat block and leave on the benchtop to cool to room temperature.
6. Reset the heat block to 37 °C.
7. Prepare 1.5 μg/μl Cas9 protein working solution. Mix the following reagents by flicking the tube and spin down briefly. Do not vortex.

Component	Volume (μl)
10ug/ul Alt-R® S.p.HiFi Cas9 Nuclease V3	1.5
Cas9 working buffer	8.5
Final volume	10

The volumes provided here are the optimized results generated in our experiments (see Section 4.3). The user can adjust the volumes as required.

8. Assemble the CRISPR-Cas9 RNP complexes. For each experimental group, combine 3 μl of 9 μM gRNA working solution with 3 μl of 1.5 μg/μl Cas9 protein working solution. Mix the reagents by flicking the tube and spin down briefly. Do not vortex.
9. Incubate the CRISPR-Cas9 RNP complexes at 37 °C for 10 min.
10. Remove the CRISPR-Cas9 RNP complexes from the heat block and leave on the benchtop to cool to room temperature.

NOTE:

- Keep the whole process RNase-free. Clean work surfaces with RNase-inactivating solution, handle all materials with gloves and use RNase-free tips and tubes.
- In this protocol we used HiFi Cas9 nuclease, which has significantly reduced off-target effects compare to wildtype S.p.Cas9 nuclease [22].

4.2. Microinjection

Two possible delivery strategies can be applied in embryo microinjection: inject into the single cell or the yolk sac. In theory, cell injections are more likely to induce gene editing and increase the chance of editing both alleles simultaneously. However, it is technically challenging and time-consuming, limiting the number of embryos that can be injected in a single experiment. In comparison, yolk injections are high throughput, enabling an increased number of injected embryos to be achieved in one sitting. Additionally, yolk injections have been shown to have similar mutagenesis efficiencies to single-cell injections, with four times the

reagent dose [23].

1. The afternoon before scheduled injection, set up zebrafish in breeding tanks and separate the males and females with dividers. We use two males to three females to increase the number of fertilised eggs produced for injection.
2. On the morning of injection, pull out the dividers and allow the fish to spawn naturally. After approximately 10–15 min, collect the embryos and inject 1 nl of the CRISPR-Cas9 RNP into the cell of each one-cell stage embryo or 4 nl into the yolk sac instead. Use forceps to gently remove the embryos that have divided past the single-cell stage or fail to be injected. Save uninjected embryos from each clutch as controls.
3. Incubate both injected and uninjected embryos at 28.5 °C in E2 media with Methylene Blue in petri dishes. After 4–6 h, remove unfertilized or dead eggs, refresh the E2 media and record the number of surviving embryos. From 24hpf, raise the embryos in 1x PTU egg water to suppress pigment formation. Change the 1x PTU egg water twice a day as well as remove any dead embryos. Check and record the survival and dysmorphic rates. The injected larvae can be assessed for cataract and collected for editing efficiency analysis at 4dpf.

NOTE:

- Inject embryos as soon as possible and not beyond the one-cell stage. Early injection maximizes editing and reduces the genetic mosaicism, making the subsequent evaluation of editing efficiency easier.
- It is recommended to line up and orient the embryos before injection. This can speed up the injection process when performing cell injections, and avoids accidentally injecting the relatively large amount of CRISPR-Cas9 RNP (4 nl) into the cell when performing yolk injections.
- The injection should be a single smooth motion. Do not adjust the orientation of the needle in the embryo. After injecting the RNP complexes, gently withdraw the needle and avoid tear out of the cytoplasm or yolk sac.
- Power calculations should be performed to determine the minimum number of injected embryos required for statistical analysis. Inject more embryos than required to allow for natural attrition of early embryos. The number can be based on the survival rate calculated from optimization experiments.
- In general, more than 50% of the embryos in the injected group are expected to show normal development similar to the uninjected siblings.
- High levels of embryo death may be caused by excessive reagent concentration or may indicate that the target gene is essential for embryo survival. Repeat injections with a decreased reagent concentration.
- Cloudy yolk sacs in surviving embryos likely indicate infection. Rinse the embryos carefully with E2 media prior to injection to remove any debris. Timely removal of dead embryos also helps to maintain the health of remaining embryos.

4.3. Optimization of dose and delivery route of CRISPR-Cas9 RNP

To achieve the optimal editing efficiency with minimum disruption to the development of the zebrafish embryo, we used gRNA targeting *tyrosinase (tyr)* gene to optimize the dose and delivery route of CRISPR-Cas9 RNPs. Knockout of the *tyr* gene results in pigmentation defects, which can be easily observed as early as 2 dpf (Fig. 2A) and quantitatively analyzed by measuring the pigment areas on the retina and the body of the injected zebrafish (Figure S1). *tyr*-gRNA is commercially available from IDT, or it can be designed by the user through the web-based CRISPR design tools. In the initial dose optimization process, the reagents were injected into the cell of one-cell-stage embryos at a fixed volume of 1 nl. We first tested a range of gRNA concentrations from 0.5 μM to 13.5 μM, while keeping Cas9 nuclease at 0.75 μg/μl. A significant reduction of pigmentation in the retina and body were observed in 4.5 μM and 13.5 μM gRNA-injected zebrafish (Fig. 2B and C). However, no statistical difference in pigment loss was found between 4.5 μM and 13.5 μM gRNA-injected zebrafish (retina: $p = 0.9427$; body: $p = 0.9356$). We then applied 4.5 μM and 13.5 μM gRNA to examine the effect of varying Cas9 concentration at 0.75 μg/μl or 1 μg/μl. In all experimental conditions that tested in the Cas9 concentration optimization, we observed significant pigment loss on both retina and body in the injected groups compared with the uninjected group (Fig. 2D and E), indicating high mutagenesis load. Although there were no significant differences in pigment loss between the injected groups in the optimization of Cas9 concentration (data not shown), the combination of 4.5 μM gRNA and 0.75 μg/μl Cas9 nuclease presented with the highest survival rates (93%, 57 of 61 injected embryos). We therefore set the concentration of gRNA and Cas9 nuclease to be 4.5 μM and 0.75 μg/μl.

We next used this condition to determine the delivery route. With the identical concentration of gRNA and Cas9 nuclease, we compared the pigment loss of injecting 1 nl of CRISPR-Cas9 RNP into the cell (Fig. 3A) and 4 nl into the yolk (Fig. 3B) of one-cell stage embryos. Our data showed that yolk injections had significantly higher body pigment loss (Fig. 3D, $p = 0.042$) and slightly higher survival rate (cell: 73%, 19 of 26 injected embryos; yolk: 88%, 30 of 34 injected embryos) than cell injections. In addition, considering the simple operation and high throughput of yolk injection, we chose to perform yolk injections in all subsequent experiments.

4.4. Analysis of editing efficacy in F0 embryos:

According to the principles described in Section 4.1.1, we designed 4 gRNAs targeting different locations of *HTR1Fa* exon 2 and *HTR1Fb* exon 1 respectively (Figure S2 and S3, Table S1). We first injected embryos with individual gRNAs and analyzed the editing efficiency. A detailed protocol of the single gRNA editing efficacy analysis is presented below. To improve consistency and convenience, we employed Phire Tissue Direct PCR Master Mix kit in the target region amplification step.

1. Collect 5 larvae from each gRNA injected group at 4pdf, amplify the gRNA target region of individual larvae using the Phire Tissue Direct PCR Master Mix kit according to the manufacturer's instructions.
2. After PCR, inspect the PCR products on a 2% (w/v) gel to confirm that the target region has been amplified correctly, then Sanger sequence the amplicons.
3. Upload the Sanger sequencing data (AB1 file) of both experimental and uninjected wildtype samples to the free online CRISPR analysis tool — Inference of CRISPR Edits (ICE) (https://www.synthego.com/products/bioinformatics/crispr-analysis) and specify the guide sequence. Once all the samples have been uploaded, click "Analyze" to perform the CRISPR editing efficiency analysis.

The 8 designed gRNAs displayed various editing efficiencies, with the average indel percentage of individual embryos ranging from 53.4% to 88.4% (Fig. 4). We next pooled all 8 gRNAs at equal concentrations and co-injected the gRNA mixture with Cas9 nuclease into the embryos. Although a high survival rate was observed (87%, 68 of 78 injected embryos), a high dysmorphic rate (54%, 20 of 37 imaged embryos) was also observed in the injected embryos, suggesting 8 gRNAs may be too toxic to the development of embryos. We then injected CRISPR-Cas9 RNPs carrying a mixture of the two most efficient gRNAs of both *HTR1F* orthologs into the embryos. The four-gRNA injected embryos showed a similar survival rate (78%, 58 of 74 injected embryos) to the eight-gRNA ones, but the dysmorphic rate (12%, 7 of 58 imaged embryos) decreased dramatically to an acceptable level.

NOTE:

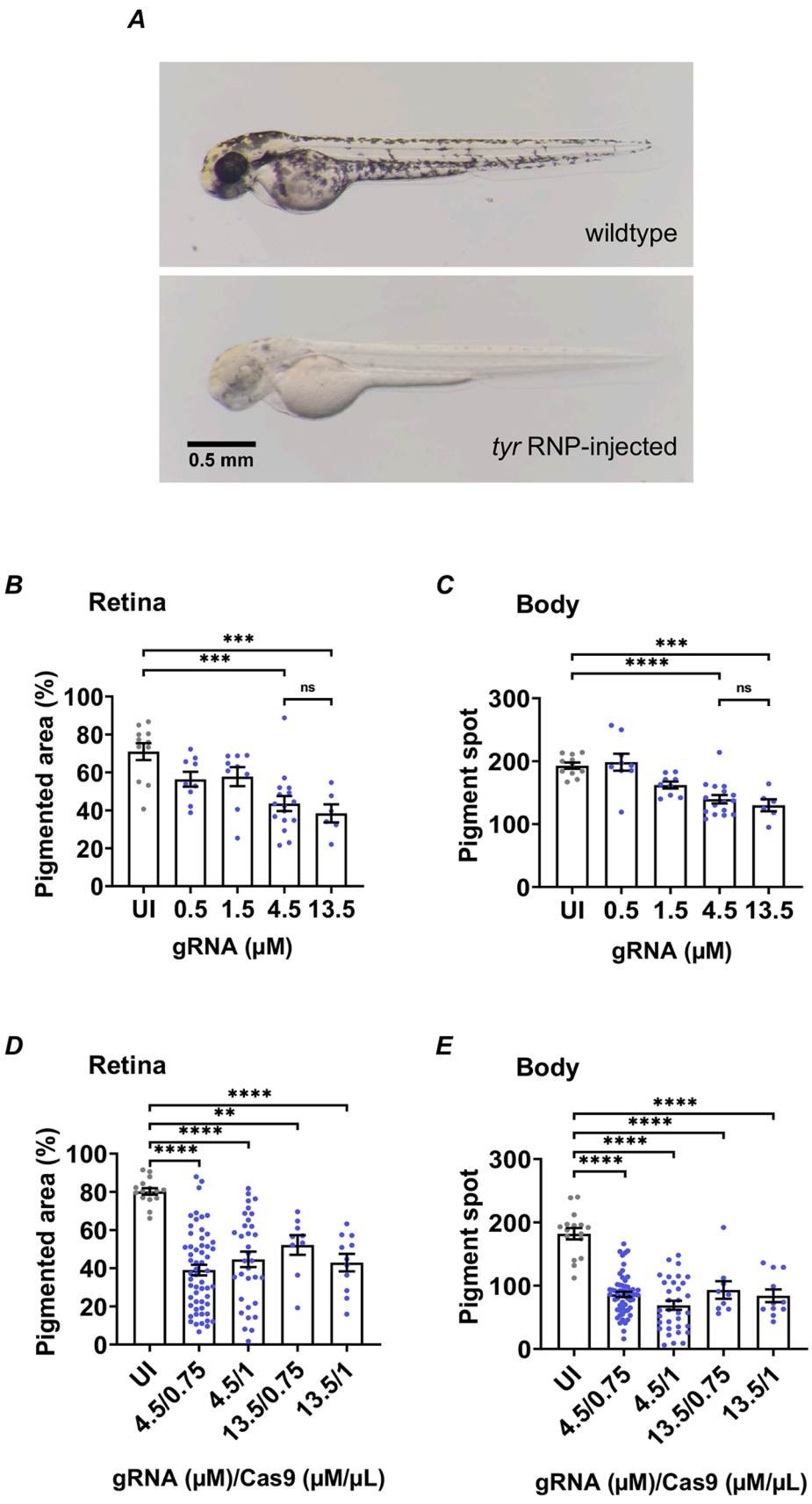

Fig. 2. CRISPR-Cas9 RNP dose optimization. A. Zebrafish embryos at 2dpf. Embryos injected with CRISPR-Cas9 RNP against *tyr* gene (bottom) had observable pigment loss compare to uninjected wildtype zebrafish (top). B and C. Optimization of *tyr* gRNA concentration (UI: n = 11, 0.5 μM: n = 9, 1.5 μM: n = 9, 4.5 μM: n = 16, 13.5 μM: n = 6). D and E. Optimization of Cas9 concentration (UI: n = 16, 4.5 μM/0.75 μg/μl: n = 57, 4.5 μM/1μg/μl: n = 33, 13.5 μM/0.75 μg/μl: n = 9, 13.5 μM/1μg/μl: n = 11). The pigment areas on the retina (B, D) and body (C, E) of zebrafish injected with a series of different concentrations of *tyr* gRNA or Cas9 were measured and compared (UI: uninjected; $^{**}p < 0.01$, $^{***}p < 0.001$, $^{****}p < 0.0001$; ns: not significant; one-way ANOVA and Tukey's multiple comparisons test; Mean ± SEM).

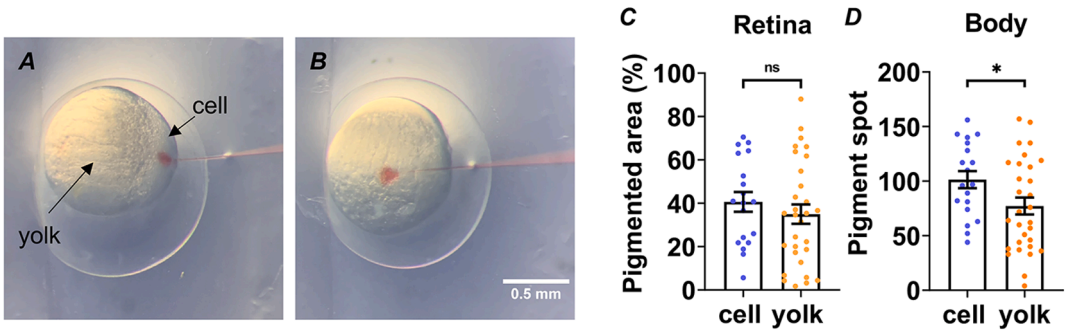

Fig. 3. CRISPR-Cas9 RNP delivery route optimization. A and B. Illustrations of cell injection (A) and yolk injection (B). The zebrafish embryos were cell-injected (n = 19) or yolk-injected (n = 30) with *tyr* RNP. The pigment areas on the retina (C) and body (D) of zebrafish in the cell injection group and yolk injection group were measured and compared. (*p < 0.05, ns: not significant; unpaired two-tailed *t*-test; Mean ± SEM).

- Alternative methods for assessing genome editing include T7E1 assay [24], high-resolution melting analysis (HRMA) [25], heteroduplex mobility assay (HMA) [26], CRISPR-STAT assay [27], and next-generation sequencing (NGS) [28].
- In the case of multi-guide-induced complex editing, we recommend applying NGS for editing efficacy analysis. ICE cannot clearly distinguish between noise and sample signal less than 5%, cannot detect deletions >150 bp for a multi-guide experiment, and can only analyze up to 3 gRNAs for the multi-guide knockout.
- When amplifying the target region to detect mutagenesis activities that are induced by multiple gRNAs, properly design primer pairs to capture all gRNA target sites in a single amplicon, otherwise deletions generated between targets will remove primer binding sites and prevent PCR based amplification.

4.5. Evaluation of cataract formation by microscope imaging

4.5.1. Imaging

1. On the fourth day after injection, anesthetize the larvae in tricaine (300 mg/l) for 1–2 min.
2. Transfer a single larva to a glass base dish (27 mm diameter).
3. Take whole-embryo images to record the gross morphology of the larvae. Our lab uses an SZX16 zoom stereomicroscope with Mightex S-Series compact USB 2.0 camera and SSClassicCamera software.
4. Mount the larva in 0.5% (w/v) agarose and quickly orient it to a position in which the lens can be viewed directly through the bottom of the dish before the agarose hardens.
5. Photograph the lens of the mounted larva using Differential Interference Contrast (DIC) microscopy settings with a Ti live cell microscope, Zyla 4.2 PLUS sCMOS camera and NIS-Elements AR acquisition software (or equivalent). Label the images with the fish number, experiment group and the time of imaging.

NOTE:

- Keep the melted agarose at approximately 40 °C, avoiding too high or too low temperatures. High temperatures will damage the larva, while low temperatures will cause the agarose to set too quickly, without allowing enough time to orient the larva.
- Remove as much liquid as possible from the larva before mounting to prevent the larva from floating in the liquid and not being fixed.
- Carefully wipe the glass bottom of the dish every time before mounting the larva, as any dirt or droplets on the dish bottom will be photographed into the lens images and interfere with the subsequent assessment of cataract.
- Position the larva with one eye facing and touching the bottom of the dish. Avoid bubbles or agarose between the larva eye and the dish bottom, which will create artefacts or blur the lens image, making cataract assessment difficult.

4.5.2. Cataract assessment

The lens images were used to determine the cataract status of each fish. There are currently no standard criteria for the characterization of cataracts in zebrafish models. The difficulties in cataract assessment of zebrafish are mainly focused on the identification of normal developing

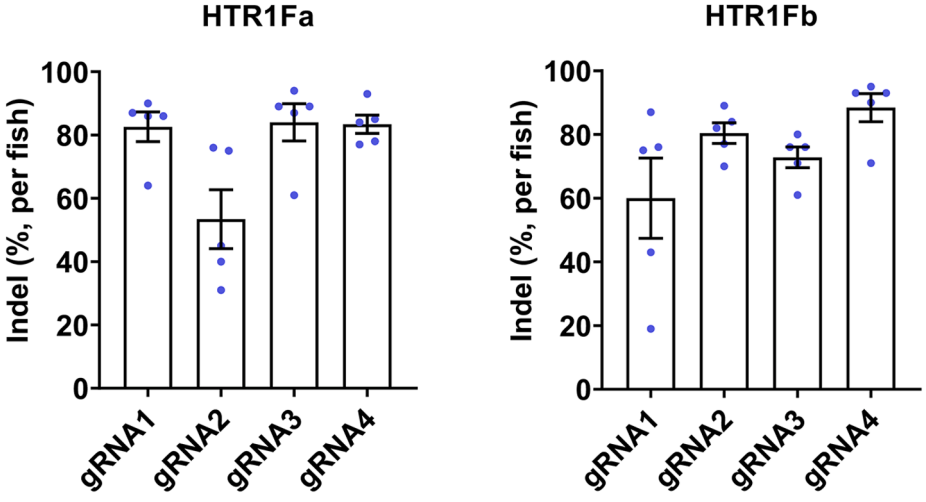

Fig. 4. Editing efficiency analysis for individual gRNA. 5 injected larvae were randomly selected at 4dpf from each gRNA injected group, and the target region of individual embryos was amplified and analyzed for indel percentage.

lenses and artefacts from real cataracts. We reviewed the literature on the developing zebrafish lens morphology [29–33] as well as studies of cataract in zebrafish models [32,33], and reviewed the lens images produced from wildtype (uninjected) embryos from our experiments to understand the morphology of normal developing zebrafish lens. We then generated a detailed cataract assessment and scoring criteria for zebrafish models based on more than 700 lens images obtained from our experiments (Fig. 5 and Fig. 6).

1. Crop lens images in ImageJ [34] to display only the lens region of the eye to avoid calling bias based on the phenotype of surrounding ocular features.

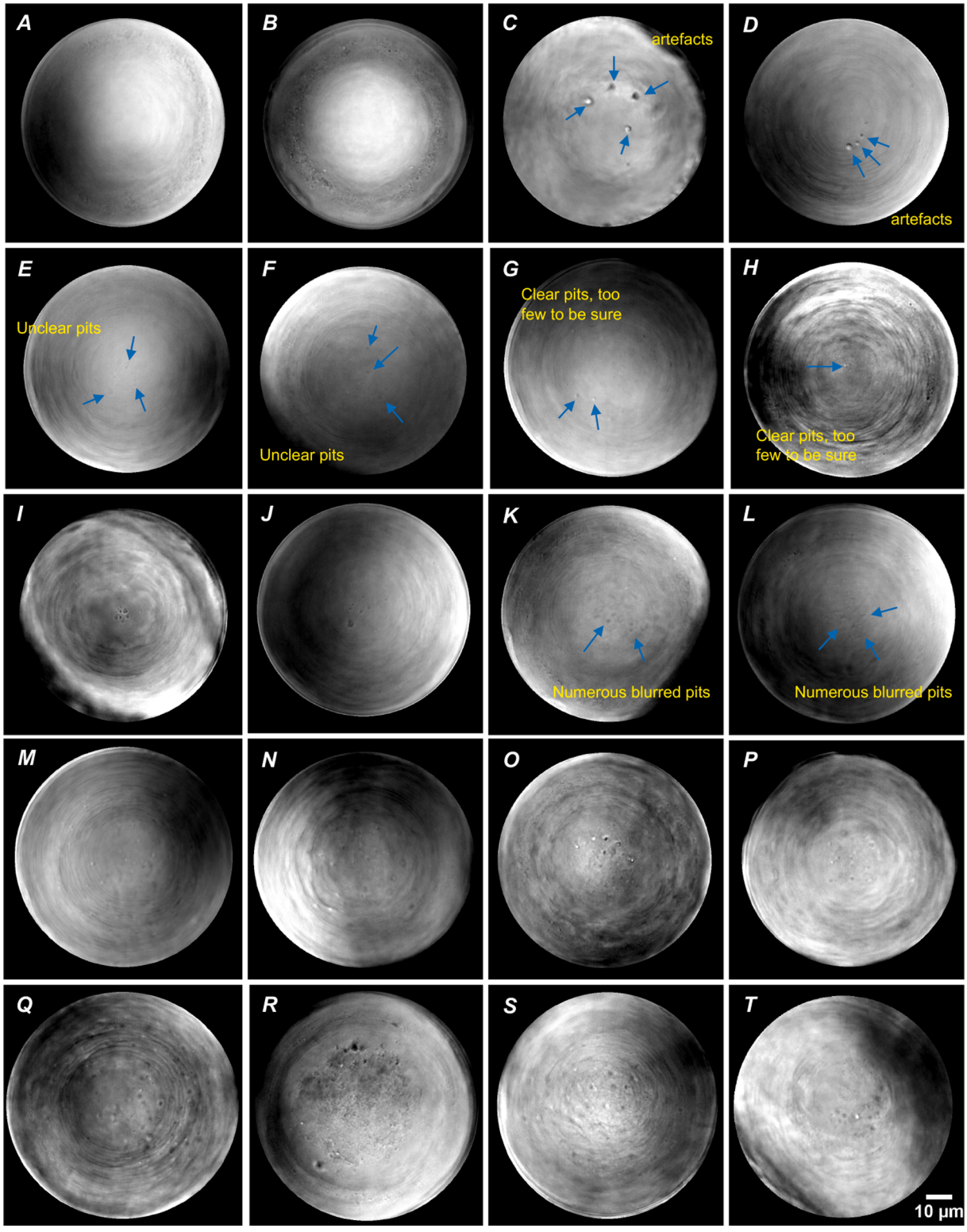

Fig. 5. Zebrafish cataract assessment criteria (pitting).

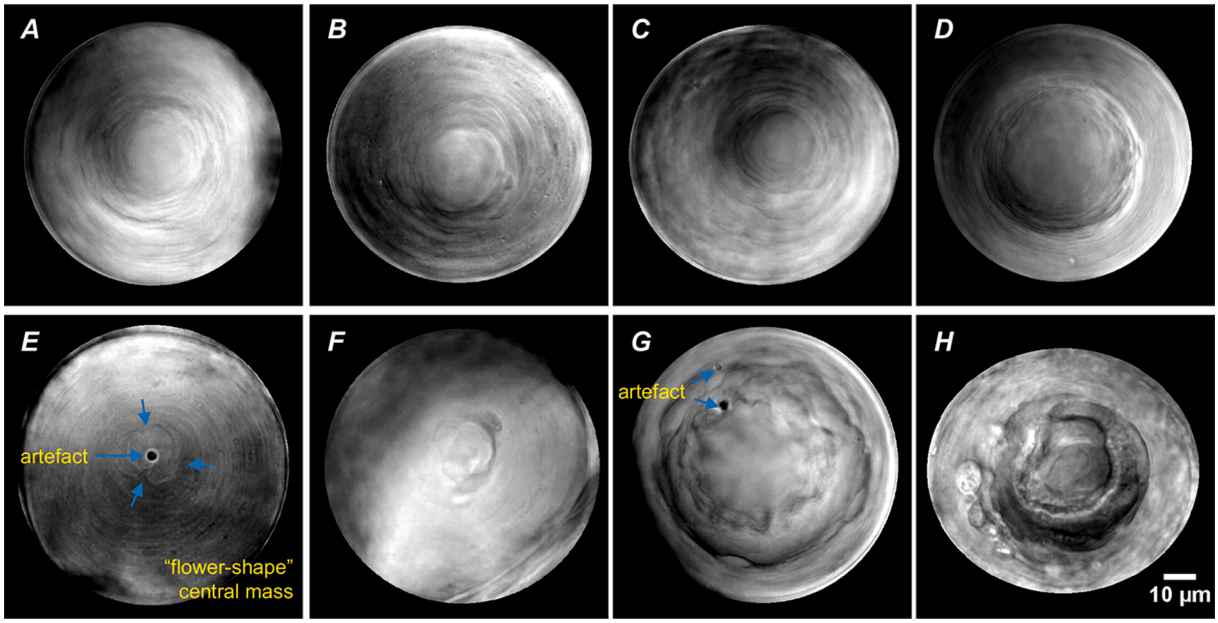

Fig. 6. Zebrafish cataract assessment criteria (central mass).

2. Collate all images into a single group-set and perform blinding using a random number generator, to randomise and reassign image identification numbers.
3. Provide the blinded data to two researchers who should independently assess and score the images based on the standard images in Fig. 5 and Fig. 6 and descriptions below.

- **Pitting.** Described as a dot-shaped depression on the surface of the lens. The pits can be diffused or aggregated in the central lens. Where pits exist, the uniform and smooth structure of the lens is destroyed.

Catagory	Description
Pitting = No/ cataract = No	Can be: • Developmental pitting (Fig. 5A and B). The pits are mostly fine and spread over the outer lens. They are undegraded organelles. The central lens is clear and uniform. • Artefacts (Fig. 5C and D). High reflective pits with very round and regular shape or pits with blurred edges are considered to be artefacts. The central lens is clear and uniform.
Pitting=?/ cataract = No	Can be: • Unclear pits (Fig. 5E and F), few in number in the centre of the lens. The rest of the lens is smooth and uniform. • Clear pits, but too few to be sure (Fig. 5G and H). There are one or two clear pits in the centre of the lens. The rest of the lens is smooth and uniform.
Pitting = Yes/ cataract = Yes (mild, score = 1)	Can be: • A small number of clear pits, enough to be confident (Fig. 5I and J). The pits are located in the central lens rather than the outer lens. • Pits may be blurred, but are numerous in the central lens (Fig. 5K and L). This may be caused by loss of focus during imaging.
Pitting = Yes/ cataract = Yes (moderate, score = 2)	Significant pits (Fig. 5M-P). Can be seen all over the lens or cluster in the central lens.
Pitting = Yes/ cataract = Yes (severe, score = 3)	Significant pits, deep or high density (Fig. 5Q-T). Seriously obstruct the visual pathway.

- **Central mass.** The centre of the lens presents as an irregular shape protrusion, which is significantly different from the rest of the lens. The central lens has lost its smooth and high regular structure.

Catagory	Description
Central mass = No/ cataract = No	The centre of the lens may seem to bulge out compared to the rest of the lens, but it is smooth, uniform and has a regular shape (Fig. 6A-D). The outer lens is uniform and well developed. This could be an optical illusion caused by light or the different depths of the lens that had been captured during imaging.
Central mass = Yes/ cataract = Yes (mild, score = 1)	The central lens lost its round shape and become "flower-shape" (Fig. 6E). The outer lens is mostly uniform and well developed. The "flower-shape" is presumed to be the outline of the original, undifferentiated cells in the lens nucleus.
Central mass = Yes/ cataract = Yes (moderate, score = 2)	The central lens is abnormal, lost its round shape and smooth, uniform texture (Fig. 6F). In the lens nucleus, original, undifferentiated cells appear to be visible, meanwhile the outer lens is well developed.
Central mass = Yes/ cataract = Yes (severe, score = 3)	The central lens is significantly abnormal, completely lost its regular, smooth texture (Fig. 6G and H).

4. Any images with differing cataract classifications should then be assessed by a third researcher to break the tie, prior to unblinding.

NOTE:

- Frequently, regular concentric circles (Fig. 7A and B) or irregular "ring-like" (Fig. 7C-E) or "wave-like" structures (Fig. 7F-H) can be observed in the lenses with the central area uniform and smooth. They are believed to be maturing lens fiber cells rather than developmental cataracts, as we observed similar structures in the lens images of developing wildtype zebrafish that showed in the literature [29–33]. No cataract is called unless there is obvious disruption to make the "flower-shape" that is highlighted in the central mass category.

5. Discussion

Gene identification for inherited paediatric cataract continues and has accelerated in recent years with the advent of whole exome and

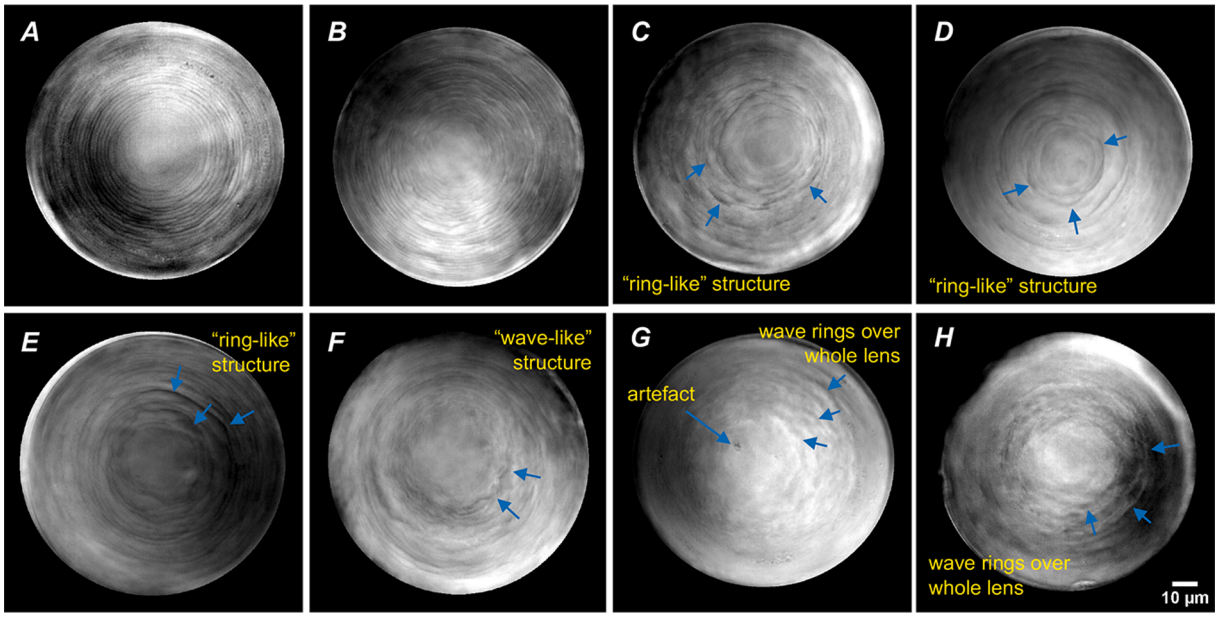

Fig. 7. Normal developing lens images with maturing lens fiber cells.

genome sequencing to complement family-based linkage approaches. However, functional validation of these genes remains a bottleneck in the discovery pipeline. The rapid development of genome engineering techniques, particularly CRISPR-Cas9, has greatly promoted reverse genetic screening, making routine functional assessment possible. Here we provide a step-by-step protocol as well as hands-on tips for rapid and highly efficient evaluation of cataract candidate genes in F0 zebrafish using a CRISPR-Cas9 RNP strategy. We generated zebrafish cataract assessment criteria, which to our knowledge, are the first systematic, definitive cataract assessment criteria for the zebrafish model. This protocol can be used to develop zebrafish models for in-depth study of specific genes, or to rapidly assess the cataract forming potential of multiple genes. With gene discovery in human patients and their families routinely employing genome-wide approaches, it is not uncommon to identify several plausible candidate genes. Ideally, similar variants in those genes would be found in additional affected families, however, that process can take many years until just the right family makes it into a research or diagnostic program. The use of a rapid zebrafish-based functional validation protocol can provide valuable evidence for the role of candidate genes in cataract formation.

A major concern of the F0-based gene functional evaluation is the genetic mosaicism in the injected fish. The variety of unpredictable indels induced by CRISPR-Cas9 complicate phenotypic analysis. However, some recent studies have demonstrated that well-designed CRISPR-Cas9 with mutagenesis efficiency approaching saturation can induce almost fully penetrant loss-of-function phenotypes with low off-targets, faithfully simulating the null mutants in F0 embryos [21,23,35,36]. Several critical strategies were applied in our protocol to maximize mutagenesis efficiency. Firstly, we provide comprehensive gRNA design instructions and detailed injection condition optimization pipeline to obtain appropriately designed guides and optimal injections, thus lay the foundation for high mutagenesis efficiency. In our hands, five of the eight tested gRNAs had an editing efficiency of over 80%, with the maximum editing efficiency reached 88.4%. Secondly, by designing gRNAs targeting multiple sites of a single gene and injecting these gRNAs simultaneously, the mutagenicity is further improved with the increase of the probability of including efficient guides and loss-of-function deletions. Finally, we applied CRISPR-Cas9 RNP, which is more mutagenic compare to the CRISPR-Cas9 mRNA complex [18,21], to achieve saturating mutagenesis. After successful evaluation following this protocol, any promising cataract candidates can be further confirmed in stable germline-transmitted mutant lines.

Another vital factor for successful cataract candidate gene evaluation is the accurate identification of cataract phenotypes in the fish lens. Because of its simplicity and directness, lens images of live embryos are widely used for phenotypic assessment of zebrafish cataract models. However, there is a lack of standardized reference material available to assess zebrafish cataract development. Multiple factors can interfere with the cataract assessment. Developmental delays are frequently observed in CRISPR-Cas9 injected embryos, and the presence of developing lens fiber cells makes it difficult to distinguish real cataracts. A similar study reported that cataracts detected at 3dpf were absent at 4dpf [37]. It cannot be ruled out that the phenotypes observed are the manifestation of immature lenses and not developmental cataracts. Therefore, we suggest analysing the phenotype at 4dpf or even 5dpf, to ensure the lens is of sufficient maturity to obtain reliable phenotypes. Artefact is another confounding factor. Based on our experience, lesions with a very round and regular shape, highly reflective dots or pitting with blurred edges are considered artefacts. In addition, CRISPR injection itself is possible to lead to non-specific lens lesions. In this situation, the false positive phenotypes can be effectively eliminated by the use of a properly designed negative control such as *LacZ*. In our assessment criteria, we defined cataract in the early zebrafish larvae by characterizing defects that lead to gross changes in lens morphology observable by brightfield microscopy with further classification by severity. Examples of false positives are also given. Our use of single fish strain (AB) and a mild phenotype observed with our chosen candidate gene are the major limitations of our cataract assessment criteria to date. These should continue to be developed to apply to additional strains which may have different developmental rates and to account for more severe cataract that may be observed with different genes.

In summary, we report a simple CRISPR-Cas9 RNP based method for rapid and efficient evaluation of cataract candidate genes in F0 zebrafish. Compared with traditional functional analysis strategies that need to establish stable mutant lines, our protocol creates significant labour- and time-savings. In addition, we also generated detailed criteria to allow standardized assessment of the lens phenotype using brightfield imaging and provide reference images for accurate and rigorous phenotypic analysis.

Declaration of Competing Interest

The authors declare that they have no known competing financial

interests or personal relationships that could have appeared to influence the work reported in this paper.

Acknowledgement

We thank Elise Yeaman for technical support and maintenance of zebrafish lines.

Funding

This work was supported by the National Health and Medical Research Council (NHMRC) of Australia [grants GNT1185477, GNT1059954 and GNT1116360]. Duran Zhao was supported by a Health Tasmania Graduate Research Scholarship.

Appendix A. Supplementary data

Supplementary data to this article can be found online at https://doi.org/10.1016/j.ymeth.2020.12.004.

References

[1] S.R. Flaxman, R.R. Bourne, S. Resnikoff, P. Ackland, T. Braithwaite, M.V. Cicinelli, et al., Global causes of blindness and distance vision impairment 1990–2020: a systematic review and meta-analysis, Lancet Global Health 5 (12) (2017) e1221–e1234.
[2] L. Zhao, X.-J. Chen, J. Zhu, Y.-B. Xi, X. Yang, L.-D. Hu, et al., Lanosterol reverses protein aggregation in cataracts, Nature 523 (7562) (2015) 607–611.
[3] J.F. Hejtmancik, Congenital cataracts and their molecular genetics, Semin. Cell Dev. Biol. 19 (2008) 134–149.
[4] A. Shiels, T.M. Bennett, J.F. Hejtmancik, Cat-Map: putting cataract on the map, Mol. Vision 16 (2010) 2007.
[5] A. Shiels, J.F. Hejtmancik, Mutations and mechanisms in congenital and age-related cataracts, Exp. Eye Res. 156 (2017) 95–102.
[6] R.L. Gillespie, J. O'Sullivan, J. Ashworth, S. Bhaskar, S. Williams, S. Biswas, et al., Personalized diagnosis and management of congenital cataract by next-generation sequencing, Ophthalmology 121 (11) (2014), 2124–2137.e2.
[7] S. Javadiyan, J.E. Craig, E. Souzeau, S. Sharma, K.M. Lower, D.A. Mackey, et al., High-throughput genetic screening of 51 pediatric cataract genes identifies causative mutations in inherited pediatric cataract in South Eastern Australia, G3: Genes, Genomes, Genetics 7 (10) (2017) 3257–3268.
[8] A.S. Ma, J.R. Grigg, G. Ho, I. Prokudin, E. Farnsworth, K. Holman, et al., Sporadic and familial congenital cataracts: Mutational spectrum and new diagnoses using next-generation sequencing, Hum. Mutat. 37 (4) (2016) 371–384.
[9] P. Goldsmith, Modelling eye diseases in zebrafish, NeuroReport 12 (13) (2001) A73–A77.
[10] G.J. Lieschke, P.D. Currie, Animal models of human disease: zebrafish swim into view, Nat. Rev. Genet. 8 (5) (2007) 353.
[11] K. Howe, M.D. Clark, C.F. Torroja, J. Torrance, C. Berthelot, M. Muffato, et al., The zebrafish reference genome sequence and its relationship to the human genome, Nature 496 (7446) (2013) 498–503.
[12] W.Y. Hwang, Y. Fu, D. Reyon, M.L. Maeder, S.Q. Tsai, J.D. Sander, et al., Efficient genome editing in zebrafish using a CRISPR-Cas system, Nat. Biotechnol. 31 (3) (2013) 227.
[13] N. Chang, C. Sun, L. Gao, D. Zhu, X. Xu, X. Zhu, et al., Genome editing with RNA-guided Cas9 nuclease in zebrafish embryos, Cell Res. 23 (4) (2013) 465–472.
[14] P.D. Hsu, E.S. Lander, F. Zhang, Development and applications of CRISPR-Cas9 for genome engineering, Cell 157 (6) (2014) 1262–1278.
[15] S. Vivekanandan, M.F. Lou, Evidence for the presence of phosphoinositide cycle and its involvement in cellular signal transduction in the rabbit lens, Curr. Eye Res. 8 (1) (1989) 101–111.
[16] R. Boerrigter, J. Siertsema, I. Kema, Serotonin (5-HT) and the rat's eye, Doc. Ophthalmol. 82 (1–2) (1992) 141–150.
[17] M. Westerfield, The zebrafish book: a guide for the laboratory use of zebrafish, 2000 http://zfin.org/zf_info/zfbook/zfbk.html.
[18] J.A. Gagnon, E. Valen, S.B. Thyme, P. Huang, L. Ahkmetova, A. Pauli, et al., Efficient mutagenesis by Cas9 protein-mediated oligonucleotide insertion and large-scale assessment of single-guide RNAs, PLoS ONE 9 (5) (2014), e98186.
[19] S. Lessard, L. Francioli, J. Alfoldi, J.C. Tardif, P.T. Ellinor, D.G. MacArthur, et al., Human genetic variation alters CRISPR-Cas9 on- and off-targeting specificity at therapeutically implicated loci, Proc. Natl. Acad. Sci. U S A 114 (52) (2017) E11257–E11266.
[20] S. Chen, S. Sun, D. Moonen, C. Lee, A.-Y.-F. Lee, D.V. Schaffer, et al., CRISPR-READI: Efficient generation of knockin mice by CRISPR RNP electroporation and AAV donor infection, Cell Rep. 27 (13) (2019).
[21] A. Burger, H. Lindsay, A. Felker, C. Hess, C. Anders, E. Chiavacci, et al., Maximizing mutagenesis with solubilized CRISPR-Cas9 ribonucleoprotein complexes, Development 143 (11) (2016) 2025–2037.
[22] B.P. Kleinstiver, V. Pattanayak, M.S. Prew, S.Q. Tsai, N.T. Nguyen, Z. Zheng, et al., High-fidelity CRISPR–Cas9 nucleases with no detectable genome-wide off-target effects, Nature 529 (7587) (2016) 490–495.
[23] R.S. Wu, I.I. Lam, H. Clay, D.N. Duong, R.C. Deo, S.R. Coughlin, A rapid method for directed gene knockout for screening in G0 Zebrafish, Dev. Cell 46 (1) (2018) 112–25 e4.
[24] M.C. Huang, W.C. Cheong, L.S. Lim, M.H. Li, A simple, high sensitivity mutation screening using Ampligase mediated T7 endonuclease I and Surveyor nuclease with microfluidic capillary electrophoresis, Electrophoresis 33 (5) (2012) 788–796.
[25] H.R. Thomas, S.M. Percival, B.K. Yoder, J.M. Parant, High-throughput genome editing and phenotyping facilitated by high resolution melting curve analysis, PLoS ONE 9 (12) (2014), e114632.
[26] S. Ota, Y. Hisano, M. Muraki, K. Hoshijima, T.J. Dahlem, D.J. Grunwald, et al., Efficient identification of TALEN-mediated genome modifications using heteroduplex mobility assays, Genes Cells 18 (6) (2013) 450–458.
[27] G.K. Varshney, B. Carrington, W. Pei, K. Bishop, Z. Chen, C. Fan, et al., A high-throughput functional genomics workflow based on CRISPR/Cas9-mediated targeted mutagenesis in zebrafish, Nat. Protoc. 11 (12) (2016) 2357–2375.
[28] A.N. Shah, C.F. Davey, A.C. Whitebirch, A.C. Miller, C.B. Moens, Rapid reverse genetic screening using CRISPR in zebrafish, Nat. Methods 12 (6) (2015) 535–540.
[29] T.M. Greiling, J.I. Clark, Early lens development in the zebrafish: a three-dimensional time-lapse analysis, Dev. Dyn.: An Official Publication of the Am. Assoc. Anatomists 238 (9) (2009) 2254–2265.
[30] R. Dahm, H.B. Schonthaler, A.S. Soehn, J. Van Marle, G.F. Vrensen, Development and adult morphology of the eye lens in the zebrafish, Exp. Eye Res. 85 (1) (2007) 74–89.
[31] T.M. Greiling, J.I. Clark, New insights into the mechanism of lens development using zebra fish. International review of cell and molecular biology, Elsevier (2012) 1–61.
[32] N. Gath, J.M. Gross, Zebrafish mab21l2 mutants possess severe defects in optic cup morphogenesis, lens and cornea development, Dev. Dyn. 248 (7) (2019) 514–529.
[33] K. Taler, O. Weiss, S. Rotem-Bamberger, A.M. Rubinstein, P. Seritrakul, J.M. Gross, et al., Lysyl hydroxylase 3 is required for normal lens capsule formation and maintenance of lens epithelium integrity and fate, Dev. Biol. 458 (2) (2020) 177–188.
[34] J. Schindelin, I. Arganda-Carreras, E. Frise, V. Kaynig, M. Longair, T. Pietzsch, et al., Fiji: an open-source platform for biological-image analysis, Nat. Methods 9 (7) (2012) 676–682.
[35] C.J. Watson, A.T. Monstad-Rios, R.M. Bhimani, C. Gistelinck, A. Willaert, P. Coucke, et al., Phenomics-Based Quantification of CRISPR-Induced Mosaicism in Zebrafish, Cell Syst. (2020).
[36] K. Hoshijima, M.J. Jurynec, D.K. Shaw, A.M. Jacobi, M.A. Behlke, D.J. Grunwald, Highly efficient CRISPR-Cas9-based methods for generating deletion mutations and F0 embryos that lack gene function in zebrafish, Dev. Cell 51 (5) (2019).
[37] I. Vorontsova, I. Gehring, J.E. Hall, T.F. Schilling, Aqp0a Regulates Suture Stability in the Zebrafish Lens, Invest. Ophthalmol. Vis. Sci. 59 (7) (2018) 2869–2879.